

Scaling behavior of the directed percolation universality class

S. Lübeck ^{a,*}, R. D. Willmann ^b

^a*Theoretische Physik, Universität Duisburg-Essen, 47048 Duisburg, Germany*

^b*Institut für Festkörperforschung, Forschungszentrum Jülich, 52425 Jülich, Germany*

Abstract

In this work we consider five different lattice models which exhibit continuous phase transitions into absorbing states. By measuring certain universal functions, which characterize the steady state as well as the dynamical scaling behavior, we present clear numerical evidence that all models belong to the universality class of directed percolation. Since the considered models are characterized by different interaction details the obtained universal scaling plots are an impressive manifestation of the universality of directed percolation.

Key words: nonequilibrium phase transitions, universality classes, scaling functions,

PACS: 05.70.Ln, 05.50.+q, 05.65.+b

1 Introduction

In this work we consider the universality class of directed percolation (DP, see [1,2] for recent reviews). Because of its robustness and ubiquity, (including critical phenomena in physics, biology, epidemiology, as well as catalytic chemical reactions) directed percolation is recognized as the paradigm of non-equilibrium phase transitions into absorbing states. These so-called absorbing phase transitions arise from a competition of opposing processes, usually creation and annihilation processes. The transition point separates an

* Corresponding author.

Email addresses: sven@thp.uni-duisburg.de (S. Lübeck),
r.willmann@fz-juelich.de (R. D. Willmann).

active phase from an absorbing phase in which the dynamics is frozen. Analogous to equilibrium critical phenomena, absorbing phase transitions can be grouped into different universality classes. All systems belonging to a given universality class share the same critical exponents, and certain scaling functions (e.g. equation of state, correlation functions, finite-size scaling functions, etc.) become identical near the critical point. According to the universality hypothesis of Janssen and Grassberger, short-range interacting models, exhibiting a continuous phase transition into a unique absorbing state, belong to the directed percolation universality class, if they are characterized by a one-component order parameter and no additional symmetries [3,4].

Similar to equilibrium critical phenomena, the universality of directed percolation is understood by renormalization group treatments of an associated continuous field theory. The process of directed percolation might be represented by the Langevin equation [3]

$$\partial_t n(\underline{x}, t) = r n(\underline{x}, t) - u n^2(\underline{x}, t) + \Gamma \nabla^2 n(\underline{x}, t) + \eta(\underline{x}, t). \quad (1)$$

Here, $n(\underline{x}, t)$ corresponds to the density of active sites on a mesoscopic scale and r describes the distance to the critical point. Furthermore, η denotes the noise which accounts for fluctuations of $n(\underline{x}, t)$. According to the central limit theorem, $\eta(\underline{x}, t)$ is a Gaussian random variable with zero mean and whose correlator is given by

$$\langle \eta(\underline{x}, t) \eta(\underline{x}', t') \rangle = \kappa n(\underline{x}, t) \delta(\underline{x} - \underline{x}') \delta(t - t'). \quad (2)$$

Notice, that the latter equation ensures that the system is trapped in the absorbing state $n(\underline{x}, t) = 0$. Furthermore, higher order terms such as $n(\underline{x}, t)^3$, $n(\underline{x}, t)^4$ or $\nabla^4 n(\underline{x}, t)$ are irrelevant under renormalization group transformations as long as $u > 0$. Negative values of u give rise to a first order phase transition whereas $u = 0$ is associated with a tricritical point [5,6].

Above the upper critical dimension D_c mean field theories apply and present instructive insight into the critical behavior [7]. Below D_c , renormalization group techniques have to be applied to determine the critical exponents and the scaling functions (see [8,9] for recent reviews of the field theoretical treatment of directed percolation). In that case path integral formulations are more adequate than the Langevin equation. Stationary correlation functions as well as response functions can be determined by calculating path integrals with weight $\exp(-\mathcal{S})$, where the dynamic functional \mathcal{S} describes the considered stochastic process. Up to higher irrelevant orders the dynamic functional associated with directed percolation is given by [3,10–12]

$$\mathcal{S}[\tilde{n}, n] = \int d^D \underline{x} dt \tilde{n} \left[\partial_t n - (r + \nabla^2) n - \left(\frac{\kappa}{2} \tilde{n} - u n \right) n \right] \quad (3)$$

where $\tilde{n}(\underline{x}, t)$ denotes the response field conjugated to the Langevin noise field [13]. Remarkably, the above functional is well known from high energy physics and corresponds to the Lagrangian of Reggeon field theory [14]. Since DP represents the simplest realization of a nonequilibrium phase transition its field theory is often regarded as the nonequilibrium counterpart of the famous ϕ^4 -theory of equilibrium [8]. Rescaling the fields

$$\tilde{n}(\underline{x}, t) = \mu \tilde{s}(\underline{x}, t), \quad n(\underline{x}, t) = \mu^{-1} s(\underline{x}, t) \quad (4)$$

the functional S is invariant under the duality transformation (so-called rapidity reversal in Reggeon field theory)

$$\tilde{s}(\underline{x}, t) \longleftrightarrow -s(\underline{x}, -t) \quad (5)$$

for $\mu^2 = 2u/\kappa$. Note that μ is a redundant variable from the renormalization group point of view [3,15]. The rapidity reversal (5) is the characteristic symmetry of the universality class of directed percolation. It is worth to reemphasize that the rapidity reversal is obtained from a field theoretical treatment. Thus all models that belong to the universality class of directed percolation obey, at least asymptotically, the rapidity reversal after a corresponding coarse grained procedure [3]. In other words, the rapidity symmetry may not be represented in the microscopic models. For example, bond directed percolation [1] and site directed percolation [16] obey the rapidity reversal microscopically whereas e.g. the contact process and the pair contact process do not. Still, the latter two models do so asymptotically and belong to the DP class.

Due to the continuing improvement of computer hardware, high accurate numerical data of DP have become available in the last years, resulting in a fruitful and instructive interplay between numerical investigations and renormalization group analyses. In particular, investigations of the scaling behavior of the equation of state and of the susceptibility [17–19], of finite-size scaling functions [20,21], and of dynamical scaling functions [18,22] yield an impressive agreement between field theoretical and numerical results. For example, the universal amplitude ratio of the susceptibility has been calculated via ϵ -expansions [17]. In second order of ϵ , the error of the field theory estimate is about 6% for $D = 2$ (see ref. [16] for a detailed discussion). It is instructive to compare this result to the equilibrium situation. The corresponding ϕ^4 -theory value [23] differs from the exact value of the two-dimensional Ising model [24,25] by roughly 115%. Thus, in contrast to the ϕ^4 -theory the DP field theory provides excellent numerical estimates of certain universal quantities.

In our previous works we investigated the steady state critical scaling behavior of two one-dimensional models [26] and of one model in various dimensions [19], respectively. In this work we extend our investigations and consider

the steady state and dynamical scaling behavior of five different models in various dimensions. All lattice models are expected to belong to the universality class of directed percolation. So far, most works focus on the determination of the critical exponents only, neglecting the determination of universal scaling functions. It turns out that checking the universality class it is often a more exact test to consider scaling functions rather than the values of the critical exponents. While for the latter ones the variations between different universality classes are often small, the scaling functions may differ significantly [27]. Thus the agreement of universal scaling functions provides not only additional but also independent and more convincing evidence in favor of the conjecture that the phase transitions of two models belong to the same universality class. Additionally to the critical exponents and scaling functions, universality classes are also characterized by certain amplitude combinations (see e.g. [28]). But these amplitude combinations are merely particular values of the scaling functions and will be neglected in this work.

2 Lattice models of directed percolation

In the following we consider various lattice models that belong to the universality class of directed percolation. First, we revisit the contact process that is well known in the mathematical literature (see e.g. [29]). Second, we consider the Domany-Kinzel cellular automaton [30] which is very useful in order to perform numerical investigations of directed bond and directed site percolation. Third, we consider the pair contact process [31] that is characterized in contrast to the other models by infinitely many absorbing states. Unlike the first two models the universal scaling behavior of the pair contact process is still a matter of discussions in the literature. Furthermore, we briefly discuss the threshold transfer process [32] as well as the Ziff-Gularí-Barshad model [33]. The latter one mimics the catalysis of carbon monoxide oxidation.

2.1 Contact process

The contact process (CP) is a continuous-time Markov process that is usually defined on a D -dimensional simple cubic lattice (see [34] and references therein). A lattice site may be empty ($n = 0$) or occupied ($n = 1$) by a particle and the dynamics is characterized by spontaneously occurring processes, taking place with certain transition rates. In numerical simulations the asynchronous update is realized by a random sequential update scheme: A particle on a randomly selected lattice site i is annihilated with rate one, whereas particle creation takes places on an empty neighboring site with rate $\lambda N/2D$, i.e.,

$$n_i = 1 \xrightarrow{1} n_i = 0, \quad (6)$$

$$n_i = 0 \xrightarrow{\lambda N/2D} n_i = 1, \quad (7)$$

where N denotes the number of occupied neighbors of n_i . Note that the rates are defined as transition probabilities per time unit, i.e., they may be larger than one. Thus, rescaling the time will change the transition rates. In simulations a discrete time formulation of the contact process is performed. In that case a particle creation takes place at a randomly chosen neighbor site with probability $p = \lambda/(1 + \lambda)$ whereas particle annihilation occurs with probability $1 - p = 1/(1 + \lambda)$. In dynamical simulations, the time increment $1/N_a$ is associated with each attempted elementary update step, where N_a denotes the number of active sites. It is usual to present the critical value in terms of λ_c instead of p_c .

Similar to equilibrium phase transitions, it is often possible for absorbing phase transitions to apply an external field h that is conjugated to the order parameter, i.e., to the density of active sites ρ_a . Being a conjugated field it has to destroy the absorbing phase, it has to be independent of the control parameter, and the corresponding linear response function has to diverge at the critical point

$$\chi = \frac{\partial \rho_a}{\partial h} \longrightarrow \infty. \quad (8)$$

In case of the CP, the conjugated field is implemented by a spontaneous creation of particles, i.e., the external field creates a particle at an empty lattice site with rate h . Clearly spontaneous particle generation destroys the absorbing state and therefore the absorbing phase transition at all. Incorporating the conjugated field, a series of opportunities is offered to compare renormalization group results to those of numerical investigations. For example, simulations performed for non-zero field include the measurements of the equation of state [26], of the susceptibility [19], as well as of a modified finite-size scaling analysis appropriate for absorbing phase transitions [21,35].

2.2 Domany-Kinzel automaton

An important $1 + 1$ -dimensional stochastic cellular automaton exhibiting directed percolation scaling behavior is the Domany-Kinzel (DK) automaton [30]. It is defined on a diagonal square lattice with a discrete time variable and evolves by parallel update according to the following rules: A site at time t is occupied with probability p_2 (p_1) if both (only one) backward sites (at time $t - 1$) are occupied. Otherwise the site remains empty. If both backward sites are empty a spontaneous particle creation takes place with probability p_0 .

Similar to the contact process, the spontaneous particle creation destroys the absorbing phase (empty lattice) and corresponds therefore to the conjugated field h .

It is straight forward to generalize the $1 + 1$ -dimensional Domany-Kinzel automaton to higher dimensions (see e.g. [36,37,19]). In the following, we consider cellular automata on a $D + 1$ -dimensional body centered cubic (bcc) lattice where the time corresponds to the $[0, 0, \dots, 0, 1]$ direction. A lattice site at time t is occupied with probability p if at least one of its 2^D backward neighboring sites (at time $t - 1$) is occupied. Otherwise the site remains empty. This parameter choice corresponds to the probabilities $p_1 = p_2 = \dots = p_{2^D} = p$, i.e., site-directed percolation (sDP) is considered.

2.3 Pair contact process

The pair contact process (PCP) was introduced by Jensen [31] and is one of the simplest models with infinitely many absorbing states showing a continuous phase transition. The process is defined on a D -dimensional cubic lattice and an asynchronous (random sequential) update scheme is applied. A lattice site may be either occupied ($n = 1$) or empty ($n = 0$). Pairs of adjacent occupied sites, linked by an active bond, annihilate each other with probability p otherwise an offspring is created at a neighboring site provided the target site is empty. The density of active bonds ρ_a is the order parameter of a continuous phase transition from an active state to an inactive absorbing state without particle pairs. Similar to the contact process and to the Domany-Kinzel automaton a spontaneous particle creation acts as a conjugated field [26]. Since isolated particles remain inactive, any configuration containing only isolated particles is absorbing. In case of the $1 + 1$ -dimensional pair contact process with L sites and periodic boundary conditions the number of absorbing states is asymptotically given by the golden mean $N \sim (1/2 + \sqrt{5}/2)^L$ [38]. In the thermodynamic limit ($L \rightarrow \infty$), the pair contact process is characterized by infinitely many absorbing states. Due to that non-unique absorbing phase the universality hypothesis of Janssen and Grassberger can not be applied. Therefore, the critical behavior of the pair contact process was intensely investigated by simulations (including [39–43]). It was shown numerically that the critical scaling behavior of the $1 + 1$ -dimensional pair contact process is characterized by the same critical exponents [31,40] as well as by the same universal scaling functions as directed percolation [26]. In particular the latter result provides a convincing identification of the universal behavior. Thus despite the different structure of the absorbing phase, the $1 + 1$ -dimensional pair contact process belongs to the directed percolation universality class. This numerical evidence confirms a corresponding renormalization group analysis predicting DP universal behavior [44] in all dimensions. But the scaling behavior of the PCP

in higher dimension is still a matter of controversial discussions. A recently performed renormalization group analysis conjectures that the pair contact process exhibits a dynamical percolation-like scaling behavior [45,46]. A dynamical percolation cluster at criticality equals a fractal cluster of ordinary percolation on the same lattice. Thus, the dynamical percolation universality class [47–49] differs from the directed percolation universality class. In particular the upper critical dimension equals $D_c = 6$ instead of $D_c = 4$ for DP. Furthermore, the dynamical scaling behavior of the PCP is a matter of controversial discussions. Deviations from the directed percolation behavior due to strong corrections to scaling [41] as well as non-universal behavior of the exponents [50] are observed in low dimension systems.

So far, the investigations of the PCP are limited to the 1+1-dimensional [26,39–43] and 2 + 1-dimensional [51] systems. In this work we consider for the first time the PCP in higher dimensions and identify the scaling behavior via universal scaling functions.

2.4 Threshold transfer process

The threshold transfer process (TTP) was introduced in [32]. Here, lattice sites may be empty ($n = 0$), occupied by one particle ($n = 1$), or occupied by two particles ($n = 2$). Double occupied lattice sites are considered as active. In that case both particles may move to the left (l) or right (r) neighbor if possible, i.e.,

$$\begin{aligned} n_l &\longrightarrow n_l + 1 & \text{if } n_l < 2, \\ n_r &\longrightarrow n_r + 1 & \text{if } n_r < 2. \end{aligned} \tag{9}$$

Additionally to the particle movement, creation and annihilation processes are incorporated. A particle is created at an empty lattice site ($0 \rightarrow 1$) with probability r whereas a particle annihilation ($1 \rightarrow 0$) takes place with probability $1 - r$. In the absence of double occupied sites the dynamics is characterized by a fluctuating steady state with a density r of single occupied sites. The density of double occupied sites is identified as the order parameter of the process, and any configuration devoid of double occupied sites is absorbing. The probability r controls the particle density, and a non-zero density of active sites occurs only for sufficiently large values of r . In contrast to the infinitely many frozen absorbing configurations of the pair contact process, the threshold transfer process is characterized by fluctuating absorbing states. Nevertheless steady state numerical simulations of the 1 + 1-dimensional threshold transfer process yield critical exponents that are in agreement with the corresponding DP values [32]. So far, no systematic analysis of the TTP in higher dimensions was performed.

In this work we limit our investigations to the $2 + 1$ -dimensional TTP. Analogous to the $1 + 1$ -dimensional case, both particles of a given active site are tried to transfer to randomly chosen empty or single occupied nearest neighbor sites. Furthermore, we apply an external field that is conjugated to the order parameter. In contrast to the models discussed above the conjugated field can not be implemented by particle creation. Particle creation with rate h would affect the particle density, i.e., the control parameter of the phase transition. But the conjugated field has to be independent of the control parameter. Therefore, we implement the conjugated field by a diffusion-like field that acts by particle movements. A particle on a given lattice site moves to a randomly selected neighbor with probability h , if $n < 2$. Thus the conjugated field of the TTP differs from the conjugated field of the Domany-Kinzel automaton, the contact process, and the pair contact process.

2.5 Ziff-Gularí-Barshad model

Another model exhibiting a directed percolation-like absorbing phase transition is the Ziff-Gularí-Barshad (ZGB) model [33]. This model mimics the heterogeneous catalysis of the carbon monoxide oxidation



on a catalytic material, e.g. platinum. The catalytic surface is represented by a square lattice where CO or O_2 can be adsorbed from a gas phase with concentration y for carbon monoxide and $1 - y$ for oxygen, respectively. The concentration y is the control parameter of the model determining the density of the components on the catalytic surface. Adsorbed oxygen molecules dissociate at the catalytic surface into pairs of O atoms. It is assumed that the lattice sites are either empty, occupied by a CO molecule, or occupied by an O atom. Adjacent CO and O react instantaneously and the resulting CO_2 molecule leaves the system. Obviously, the system is trapped in absorbing configurations if the lattice is completely covered by carbon monoxide or completely covered by oxygen. The dynamics of the system is attracted by these absorbing configurations for sufficiently large CO concentrations and for sufficiently large O_2 concentrations. Numerical simulations show that catalytic activity occurs in the range $0.390 \lesssim y \lesssim 0.525$ [52] only. The system undergoes a second order phase transition to the oxygen passivated phase whereas a first order phase transition takes place if the CO passivated phase is approached. In particular, the continuous phase transition is expected to belong to the universality class of directed percolation [53]. This conjecture is supported by numerical determinations of certain critical exponents [52,54]. At first glance, it might be surprising that the ZGB model exhibits directed percolation like behavior since the ZGB model is characterized by two distinct

chemical components, CO and O. But the catalytic activity is connected to the density of vacant sites, i.e., to a single component order parameter [53]. Thus the observed directed percolation exponents are in full agreement with the universality hypothesis of Janssen and Grassberger. But one has to stress that the ZGB model is an oversimplified representation of the catalytic carbon monoxide oxidation. A more realistic modeling has to incorporate for example mobility and desorption processes as well as a repulsive interaction between adsorbed oxygen molecules (see e.g. [33,55]). These features affect the critical behavior and drive the experimental system out of the directed percolation universality class.

In this work, we focus on the two-dimensional ZBG model and determine certain scaling functions for the first time. Therefore, we apply an external field conjugated to the order parameter. Since the order parameter is connected to the density of vacant sites of the catalytic reaction, the conjugated field could be implemented via a desorption rate h of adsorbed oxygen molecules.

In summary, we investigate the scaling behavior of five different models spanning a broad range of interaction details, such as different update schemes (random sequential as well as parallel update), different lattice structures (simple cubic and bcc lattice types), different inactive backgrounds (trivial, fluctuating or quenched background of inactive particles), different structures of the absorbing phase (unique absorbing state or infinitely many absorbing states), as well as different implementations of the conjugated field (implemented via particle creation, particle diffusion or particle desorption). Nevertheless we will see that all models are characterized by the same scaling behavior, i.e., they belong to the same universality class.

3 Steady state scaling behavior

In this section we consider the steady state scaling behavior close to the transition point. Therefore, we performed steady state simulations of the five models described above. In particular, we consider the density of active sites $\rho_a = \langle L^{-D} N_a \rangle$, i.e., the order parameter as a function of the control parameter and of the conjugated field. Analogous to equilibrium phase transitions, the conjugated field results in a rounding of the zero-field curves and the order parameter behaves smoothly as a function of the control parameter for finite field values (see figure 1). For $h \rightarrow 0$ we recover the non-analytical order parameter behavior. Additionally to the order parameter, we investigate the order parameter fluctuations $\Delta \rho_a = L^D (\langle \rho_a^2 \rangle - \langle \rho_a \rangle^2)$ and its susceptibility χ . The susceptibility is obtained by performing the numerical derivative of the order parameter ρ_a with respect to the conjugated field (8). Similar to the

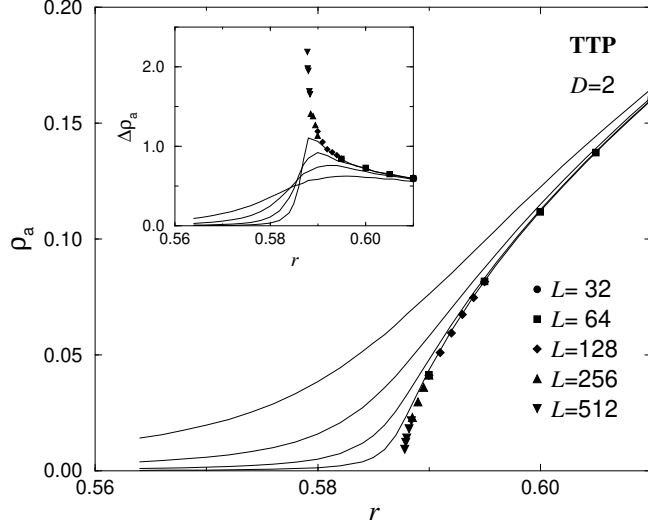


Fig. 1. The order parameter ρ_a and its fluctuations $\Delta\rho_a$ (inset) of the 2 + 1-dimensional transfer threshold process (TTP) on a square lattice for various values of the field (from $h = 10^{-5}$ to $h = 10^{-3}$). The symbols mark the zero-field behavior. The data are obtained from simulations on various system sizes with periodic boundary conditions.

equilibrium phase transitions, the fluctuations and the susceptibility display a characteristic peak at the critical point. In the limit $h \rightarrow 0$ this peak diverges, signalling the critical point.

In the following, we take only those simulation data into account where the (spatial) correlation length ξ_\perp is small compared to the system size L . In that case, the order parameter, its fluctuations, as well as the order parameter susceptibility can be described by the following generalized homogeneous functions

$$\rho_a(\delta p, h) \sim \lambda^{-\beta} \tilde{R}(a_p \delta p \lambda, a_h h \lambda^\sigma), \quad (11)$$

$$a_\Delta \Delta\rho_a(\delta p, h) \sim \lambda^{\gamma'} \tilde{D}(a_p \delta p \lambda, a_h h \lambda^\sigma), \quad (12)$$

$$a_\chi \chi(\delta p, h) \sim \lambda^\gamma \tilde{X}(a_p \delta p \lambda, a_h h \lambda^\sigma), \quad (13)$$

with the order parameter exponent β , the field exponent σ (corresponding to the gap exponent in equilibrium), the fluctuation exponent γ' , and the susceptibility exponent γ . Here, h denotes the conjugated field and δp denotes the distance to the critical point, e.g. $\delta p = (\lambda - \lambda_c)/\lambda_c$ for the contact process, $\delta p = (p - p_c)/p_c$ for site-directed percolation and for the pair contact process, $\delta p = (r - r_c)/r_c$ for the threshold transfer process, etc.. The so-called non-universal metric factors a_p , a_h , a_Δ and a_χ contain all non-universal system dependent features [56] (e.g. the lattice structure, the range of interaction, the used update scheme, as long as the interaction decreases sufficient rapidly

as a function of separation, etc.). Once the non-universal metric factors are chosen in a specified way (see below), the universal scaling functions \tilde{R} , \tilde{D} , and \tilde{X} are the same for all systems within a given universality class. The above scaling forms are valid for $D \neq D_c$. At the upper critical dimension D_c they have to be modified by logarithmic corrections [57,18].

Throughout this work we norm the universal scaling functions by $\tilde{R}(1, 0) = 1$, $\tilde{R}(0, 1) = 1$, and $\tilde{D}(0, 1) = 1$. In that way, the non-universal metric factors a_p , a_h , and a_Δ are determined by the amplitudes of the power-laws

$$\rho_a(\delta p, h = 0) \sim (a_p \delta p)^\beta, \quad (14)$$

$$\rho_a(\delta p = 0, h) \sim (a_h h)^{\beta/\sigma}, \quad (15)$$

$$a_\Delta \Delta \rho_a(\delta p = 0, h) \sim (a_h h)^{-\gamma'/\sigma}. \quad (16)$$

Taking into consideration that the susceptibility is defined as the derivative of the order parameter with respect to the conjugated field (8) we find

$$\tilde{X}(x, y) = \partial_y \tilde{R}(x, y), \quad a_x = a_h^{-1}, \quad (17)$$

as well as the scaling law

$$\gamma = \sigma - \beta. \quad (18)$$

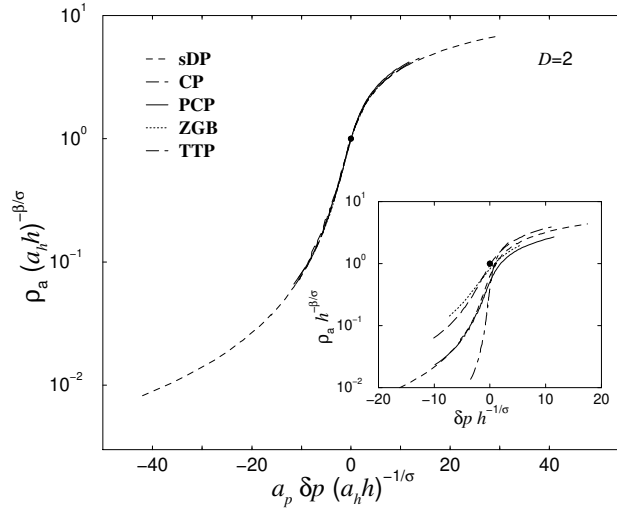


Fig. 2. The universal scaling function $\tilde{R}(x, 1)$ of the directed percolation universality class. The data are plotted according to equation (21). All models considered are characterized by the same universal scaling function, an impressive manifestation of the robustness of the directed percolation universality class with respect to variations of the microscopic interactions. Neglecting the non-universal metric factors a_p and a_h each model is characterized by its own scaling function (see inset). For all models the scaling plots contain at least four different curves corresponding to four different field values (see e.g. figure 1). The circles mark the condition $\tilde{R}(0, 1) = 1$.

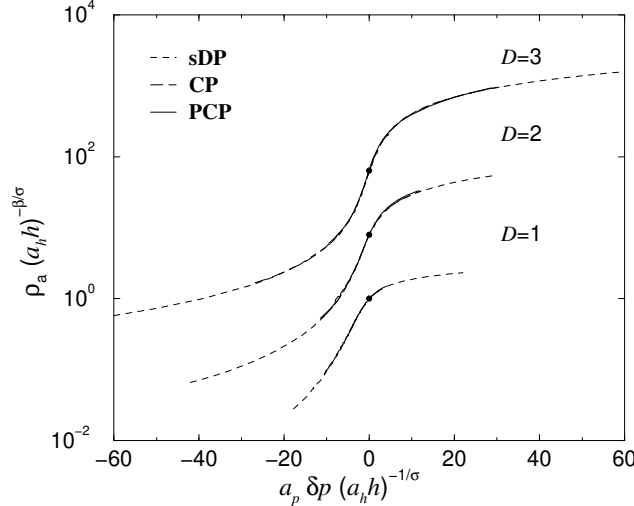


Fig. 3. The universal scaling function $\tilde{R}(x, 1)$ of the directed percolation universality class in various dimensions. The two- and three-dimensional data are vertically shifted by a factor 8 and 64 in order to avoid overlaps. The circles mark the condition $\tilde{R}(0, 1) = 1$.

This scaling law corresponds to the well known Widom law of equilibrium phase transitions. Furthermore, comparing equation (13) for $\delta p = 0$ to the definition of the susceptibility

$$a_\chi \chi(\delta p, h) \sim (a_h h)^{-\gamma/\sigma} \tilde{X}(0, 1), \quad \chi = \partial_h \rho_a = \partial_h (a_h h)^{\beta/\sigma} \quad (19)$$

leads to

$$\tilde{X}(0, 1) = \frac{\beta}{\sigma}. \quad (20)$$

This result offers a useful consistency check of the numerical estimates of the susceptibility. Furthermore, it is worth mentioning that the validity of the scaling form (11) implies the required singularity of the susceptibility (8), i.e., it confirms that the applied external field is conjugated to the order parameter.

Choosing $a_h h \lambda^\sigma = 1$ in equations (11-13) we obtain the scaling forms

$$\rho_a(\delta p, h) \sim (a_h h)^{\beta/\sigma} \tilde{R}(a_p \delta p (a_h h)^{-1/\sigma}, 1), \quad (21)$$

$$a_\Delta \Delta \rho_a(\delta p, h) \sim (a_h h)^{-\gamma'/\sigma} \tilde{D}(a_p \delta p (a_h h)^{-1/\sigma}, 1), \quad (22)$$

$$a_\chi \chi(\delta p, h) \sim (a_h h)^{-\gamma/\sigma} \tilde{X}(a_p \delta p (a_h h)^{-1/\sigma}, 1). \quad (23)$$

Thus plotting the rescaled quantities

$$\rho_a (a_h h)^{-\beta/\sigma}, \quad a_\Delta \Delta \rho_a (a_h h)^{\gamma'/\sigma}, \quad a_\chi \chi (a_h h)^{-\gamma/\sigma} \quad (24)$$

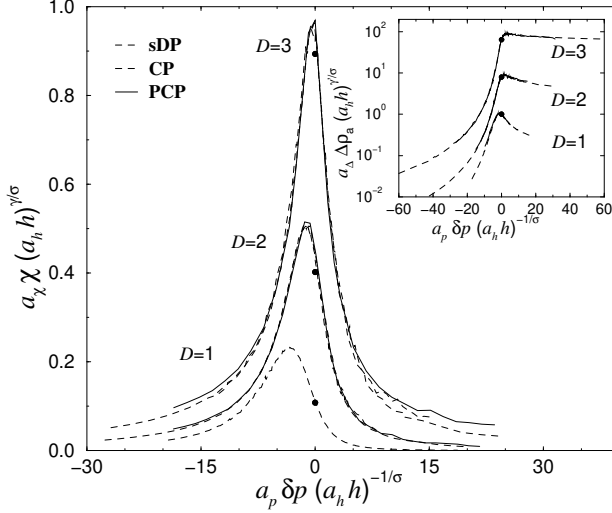


Fig. 4. The universal scaling functions of the susceptibility $\tilde{X}(x, 1)$ and of the fluctuations $\tilde{D}(x, 1)$ (inset) in various dimensions. In case of the susceptibility the two- and three-dimensional data are vertically shifted by a factor $3/2$ and $9/4$ in order to avoid overlaps. The circles mark the condition $\tilde{X}(0, 1) = \beta/\sigma$ and reflect the accuracy of the performed analysis. The two- and three-dimensional fluctuation data are vertically shifted by a factor 8 and 64 in order to avoid overlaps. The circles mark the condition $\tilde{D}(0, 1) = 1$.

as a function of the rescaled control parameter $x = a_p \delta p (a_h h)^{-1/\sigma}$ the data of all systems belonging to the same universality class have to collapse onto the universal curves $\tilde{R}(x, 1)$, $\tilde{D}(x, 1)$, and $\tilde{X}(x, 1)$. This is shown for $\tilde{R}(x, 1)$ in figure 2 where the rescaled order parameter is plotted for various two-dimensional models. For this purpose the best known estimates for the critical exponents, as given in Table 1, are used. As can be seen the data of all considered models collapse onto the same scaling function, clearly supporting the assumption that all models belong to the universality class of directed percolation. Furthermore, the data-collapse confirms the accuracy of the numerically estimated values [54] of the critical exponents.

To limit the numerical effort we skip in the following analysis the TTP and ZBG and focus to the scaling behavior of the CP, sDP, and the PCP in various dimension. The universal scaling function $\tilde{R}(x, 1)$ is displayed in figure 3 for $D = 1, 2, 3$. For each dimension, the data of the three models collapse onto the unique scaling function. As expected the scaling functions vary with the spatial dimensionality below for $D < D_c$.

The universal scaling functions of the order parameter fluctuations and the order parameter susceptibility are shown in figure 4. The susceptibility is obtained by performing the numerical derivative of the order parameter with respect to the conjugated field. The perfect data-collapses confirm the scaling forms (12,13). All scaling functions exhibit for $D = 1, 2, 3$ a clear maximum

signalling the divergence of $\Delta\rho_a$ and χ at the critical point. The susceptibility data fulfill equation (20), reflecting the accuracy of the performed analysis. In summary, all considered models are characterized by the same critical exponents and the same steady state scaling functions \tilde{R} , \tilde{D} , and \tilde{X} . Thus the steady state scaling behavior of the contact process, the Domany-Kinzel automaton, the pair contact process, the threshold transfer process, as well as of the Ziff-Gularí-Barshad model belong to the same universality class for $D = 1, 2, 3$.

3.1 Mean field regime

Mean field theories of all models considered can be simply derived and are well established (see for example [58–60,34,61,26]). These mean field theories present not only some insight into the critical behavior, they become valid above the upper critical dimension D_c . Thus analytical expressions for the scaling functions become available for $D > D_c$. In the case of directed percolation the mean-field scaling functions are given by (see e.g. [7,19])

$$\tilde{R}_{\text{MF}}(x, y) = \frac{x}{2} + \sqrt{y + \left(\frac{x}{2}\right)^2}, \quad (25)$$

$$\tilde{D}_{\text{MF}}(x, y) = \frac{\tilde{R}_{\text{MF}}(x, y)}{\sqrt{y + (x/2)^2}}, \quad (26)$$

$$\tilde{X}_{\text{MF}}(x, y) = \frac{1}{2 \sqrt{y + (x/2)^2}}, \quad (27)$$

i.e., the mean-field exponents are $\beta_{\text{MF}} = 1$, $\sigma_{\text{MF}} = 2$, $\gamma_{\text{MF}} = 1$, and $\gamma'_{\text{MF}} = 0$.

The scaling behavior of the fluctuations deserves comment. The exponent $\gamma'_{\text{MF}} = 0$ corresponds to a jump of the fluctuations and the scaling form (12) reduces to

$$a_\Delta \Delta\rho_a(\delta p, h) \sim \tilde{D}_{\text{MF}}(a_p \delta p \lambda, a_h h \lambda^\sigma). \quad (28)$$

Using again $\tilde{D}_{\text{MF}}(0, 1) = 1$, the non-universal metric factor a_Δ is determined by

$$a_\Delta = \frac{1}{\Delta\rho_a(\delta p = 0, h)}. \quad (29)$$

Numerical data of the five-dimensional models are presented in figure 5. A

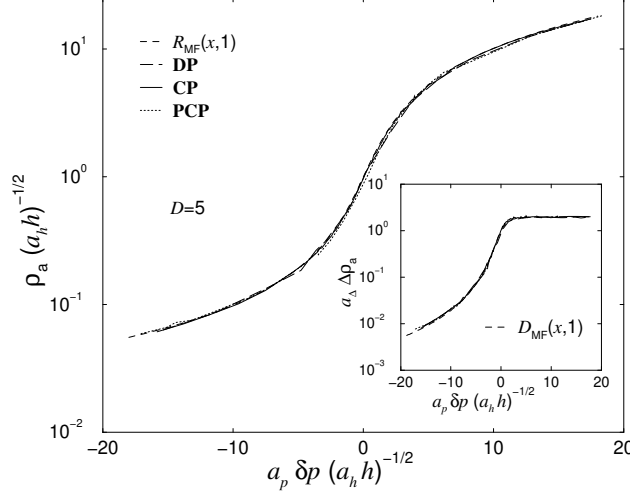


Fig. 5. The universal scaling function of the order parameter $\tilde{R}(x, 1)$ and the fluctuations $\tilde{D}(x, 1)$ (inset) for $D = 5$. The five-dimensional data agree with the corresponding mean field functions (30) and (31), respectively.

good data-collapse of the rescaled data [rescaled according to equations (21)-(23)] with the universal mean field scaling functions

$$\tilde{R}_{MF}(x, 1) = \frac{x}{2} + \sqrt{1 + \left(\frac{x}{2}\right)^2}, \quad (30)$$

$$\tilde{D}_{MF}(x, 1) = 1 + \frac{x}{2\sqrt{1 + (x/2)^2}} \quad (31)$$

is obtained.

The observed agreement of the data of the five-dimensional models with the mean field scaling functions $\tilde{R}_{MF}(x, 1)$ and $\tilde{D}_{MF}(x, 1)$ leads to the result that the upper critical dimension is less than five, in agreement with the renormalization group conjecture $D_c = 4$ [62,63]. This is a non-trivial result. The value of D_c is often predicted by field theoretical treatments, and a reliable and independent determination of the upper critical dimension is therefore of particular interest. For example, two contrary field theories conjecture for the pair contact process $D_c = 4$ [44] and $D_c = 6$ [45,46], respectively. The latter result is in clear contradiction to the observed mean field behavior in $D = 5$.

3.2 Upper critical dimension

The scaling behavior at the upper critical dimension is characterized by mean field power-laws modified by logarithmic corrections. Recent numerical investigations [64,57,19,65] as well as analytical results [18] reveal that the concept

of universal scaling functions can also be applied to the upper critical dimension. For example, the order parameter is expected to obey the scaling form (all terms in leading order)

$$a_a \rho_a(\delta p, h) \sim \lambda^{-\beta_{\text{MF}}} |\ln \lambda|^\Lambda \tilde{R}(a_p \delta p \lambda |\ln \lambda|^\Pi, a_h h \lambda^{\sigma_{\text{MF}}} |\ln \lambda|^H). \quad (32)$$

Greek capitals will be used in the following to denote the logarithmic correction exponents. According to this scaling form, the order parameter at zero field ($h = 0$) and at the critical density ($\delta p = 0$) is given by

$$a_a \rho_a(\delta p, h = 0) \sim a_p \delta p |\ln a_p \delta p|^B \tilde{R}(1, 0), \quad (33)$$

$$a_a \rho_a(\delta p = 0, h) \sim \sqrt{a_h h} \left| \ln \sqrt{a_h h} \right|^\Sigma \tilde{R}(0, 1), \quad (34)$$

with $B = \Pi + \Lambda$ and $\Sigma = H/2 + \Lambda$. Similar to $D \neq D_c$ the normalization $\tilde{R}(0, 1) = \tilde{R}(1, 0) = 1$ is used. Furthermore, the scaling behavior of the equation of state is given in leading order by

$$a_a \rho_a(\delta p, h) \sim \sqrt{a_h h} \left| \ln \sqrt{a_h h} \right|^\Sigma \tilde{R}(x, 1), \quad (35)$$

where x denotes the scaling argument

$$x = a_p \delta p \sqrt{a_h h}^{-1} \left| \ln \sqrt{a_h h} \right|^\Psi \quad (36)$$

with $\Psi = \Pi - H/2 = B - \Sigma$.

In case of directed percolation it is possible to confirm the scaling form (32) by a renormalization group analysis [18], yielding in addition the values $\Lambda = 7/12$, $\Pi = -1/4$, and $H = -1/2$. Thus the scaling behavior of the equation of state is determined by $B = \Sigma = 1/3$ and $\Psi = 0$.

Similarly to the order parameter the following scaling form is used for the fluctuations [57,19]

$$a_\Delta \Delta \rho_a(\delta p, h) \sim \lambda^{\gamma'_{\text{MF}}} |\ln \lambda|^K \tilde{D}(a_p \delta p \lambda |\ln \lambda|^\Pi, a_h h \lambda^{-\sigma} |\ln \lambda|^H). \quad (37)$$

Taking into account that numerical simulations show that fluctuations remain finite at the critical point (i.e. $\gamma'_{\text{MF}} = 0$ and $K = 0$ [19]) the scaling form

$$a_\Delta \Delta \rho_a(\delta p, h) \sim \tilde{D}(x, 1) \quad (38)$$

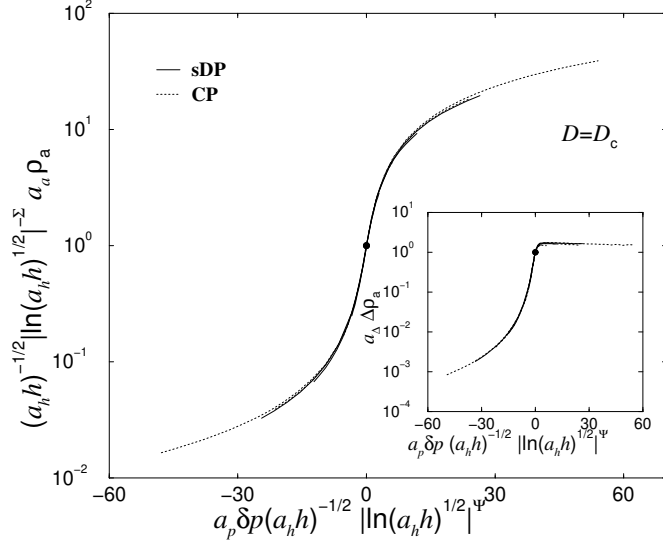


Fig. 6. The universal scaling functions of the order parameter and its fluctuations (inset) at the upper critical dimension $D_c = 4$. The logarithmic correction exponents are given by $B = \Sigma = 1/3$ [18] and $\Psi = 0$. For both models considered, the scaling plots contain at least three different curves corresponding to three different field values. The circles mark the condition $\tilde{R}(0, 1) = 1$ and $\tilde{D}(0, 1) = 1$, respectively.

is obtained, where the scaling argument x is given by equation (36) with $\Psi = 0$. The non-universal metric factor a_Δ is determined again by the condition $\tilde{D}(0, 1) = 1$.

In that way, the scaling behavior of the order parameter and its fluctuations at D_c is characterized by two exponents ($B = 1/3$ and $\Sigma = 1/3$) and four unknown non-universal metric factors (a_a, a_p, a_h, a_Δ). The detailed analysis for sDP data is described in [19]. Here we present a corresponding universal scaling plot containing data of two models, namely sDP and the CP. The corresponding scaling plots are displayed in Fig. 6 and show that the concept of universal scaling functions can be applied to the upper critical dimension.

Notice that no data-collapse is obtained if logarithmic corrections are neglected, i.e., for $B = \Sigma = 0$. Thus, at least the leading logarithmic corrections have to be taken into account in order to study steady state scaling functions. It is therefore remarkable that recently performed off-lattice simulations of the dynamical scaling behavior at $D_c = 4$ reveal that logarithmic corrections of higher orders (e.g. $\mathcal{O}(\ln \ln t)$) are necessary to describe the numerical data [66]. Although the steady state results presented here are quite convincing, we expect that even better results are obtained by incorporation higher order corrections.

4 Dynamical scaling behavior

In this section we discuss the dynamical scaling behavior close to the transition point. We limit our attention to the so-called activity spreading, generated from a single active seed. Starting with the seminal work of [67], measurements of activity spreading have been widely applied in the last two decades. In particular, they provide very accurate estimates of the critical values p_c , λ_c, \dots as well as of the exponents δ , θ , and z (see below). Here, we will focus on the scaling functions of the survival probability P_a and of the average number of active sites N_a . At criticality both quantities obey the power-laws

$$a_P P_a \sim (a_t t)^{-\delta}, \quad a_N N_a \sim (a_t t)^{\theta}, \quad (39)$$

where θ is termed the critical initial slip exponent [68]. Sufficiently close to the critical point, P_a and N_a are expected to obey the scaling forms

$$a_P P_a(\delta p, L, t) \sim \lambda^{-\delta\nu_{\parallel}} \tilde{P}_{\text{pbc}}(a_p \delta p \lambda, a_L L \lambda^{-\nu_{\perp}}, a_t t \lambda^{-\nu_{\parallel}}), \quad (40)$$

$$a_N N_a(\delta p, L, t) \sim \lambda^{\theta\nu_{\parallel}} \tilde{N}_{\text{pbc}}(a_p \delta p \lambda, a_L L \lambda^{-\nu_{\perp}}, a_t t \lambda^{-\nu_{\parallel}}), \quad (41)$$

where the time t and the system size L are incorporated as additional scaling fields. The scaling power of t has to equal the scaling power of the correlation time $\xi_{\parallel} \propto \delta p^{-\nu_{\parallel}}$, whereas the scaling power of the system size is given by the spatial correlation length exponent ν_{\perp} ($\xi_{\perp} \propto \delta p^{-\nu_{\perp}}$). In contrast to the previous section, the system size L has to be taken into account because the power-law behaviors (39) are limited by the finite system size. The index pbc indicates that the universal finite-size scaling functions depend on the particular choice of the boundary conditions as well as on the system shape (see e.g. [69–73]). But different lattice structures are contained in the non-universal metric factors.

Choosing $a_t t \lambda^{-\nu_{\parallel}} = 1$ the power-laws (39) are recovered for $\tilde{P}_{\text{pbc}}(0, \infty, 1) = 1$ as well as $\tilde{N}_{\text{pbc}}(0, \infty, 1) = 1$. The finite-size scaling forms are obtained by setting $a_L L \lambda^{-\nu_{\perp}} = 1$, yielding

$$a_P P_a(0, L, t) \sim (a_L L)^{-\delta z} \tilde{P}_{\text{pbc}}(0, 1, a_t t (a_L L)^{-z}), \quad (42)$$

$$a_N N_a(0, L, t) \sim (a_L L)^{\theta z} \tilde{N}_{\text{pbc}}(0, 1, a_t t (a_L L)^{-z}). \quad (43)$$

The scaling functions $\tilde{P}_{\text{pbc}}(0, 1, x)$ and $\tilde{N}_{\text{pbc}}(0, 1, x)$ are expected to decay exponentially for $t \gg t_{\text{FSS}}$ whereas they exhibit an algebraic behavior for $t \ll t_{\text{FSS}}$, with $t_{\text{FSS}} = a_t^{-1} (a_L L)^{\nu_{\perp}}$.

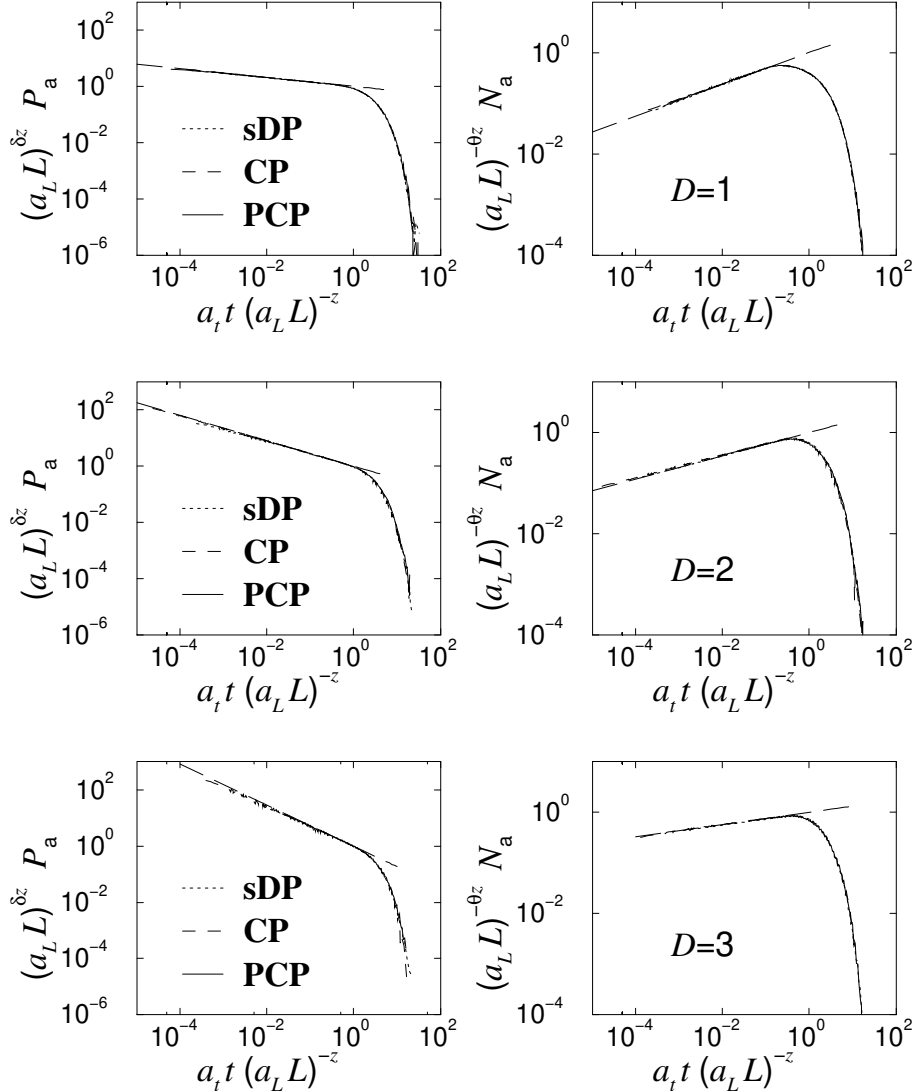


Fig. 7. The universal scaling functions \tilde{P}_{pbc} and \tilde{N}_{pbc} of activity spreading for various dimensions. In case of the pair contact process the simulations are started from a natural configuration of inactive particles. System sizes $L = 64, 128, 256, 512$ are considered for $D = 1$, $L = 64, 128, 256, 512$ for $D = 2$, and $L = 16, 32, 64, 128$ for $D = 3$. The dashed lines corresponds to the power-law behavior of the infinite system $x^{-\delta}$ and x^θ , respectively.

Performing activity spreading simulations of site directed percolation and of the contact process the initial seed is implemented by a single particle on an empty lattice. For absorbing phase transitions with non-trivial absorbing states, like the pair contact process, the scaling behavior depends upon the nature of the initial configuration [40]. In that case, spreading activity simulations have to be performed at the so-called natural density of inactive particles [40,32,35]. Starting with a random configuration, an absorbing state at criticality is prepared by the dynamics. An active seed is created for example by adding or moving a particle. The resulting activity relaxation is monitored

Table 1

The critical exponents of directed percolation for various dimensions D . In $D = 1$, the exponents γ , ν_{\perp} , and ν_{\parallel} are obtained from a series expansion by Jensen [74]. For $D = 2$ and $D = 3$ activity spreading simulations are performed yielding δ , θ , as well as z [54,75]. Additionally, the exponent ν_{\parallel} is determined [37,75] in order to estimate the full set of exponents via scaling laws.

	$D = 1$ [74]	$D = 2$ [54,37]	$D = 3$ [75]	Mean field
β	0.276486(8)	0.5834 ± 0.0030	0.813 ± 0.009	1
ν_{\perp}	1.096854(4)	0.7333 ± 0.0075	0.584 ± 0.005	1/2
ν_{\parallel}	1.733847(6)	1.2950 ± 0.0060	1.110 ± 0.010	1
σ	2.554216(13)	2.1782 ± 0.0171	2.049 ± 0.026	2
γ'	0.543882(16)	0.2998 ± 0.0162	0.126 ± 0.023	0
γ	2.277730(5)	1.5948 ± 0.0184	1.237 ± 0.023	1
δ	0.159464(6)	0.4505 ± 0.0010	0.732 ± 0.004	1
θ	0.313686(8)	0.2295 ± 0.0010	0.114 ± 0.004	0
z	1.580745(10)	1.7660 ± 0.0016	1.901 ± 0.005	2

until it ceases. Then we start a new measurement from a random configuration and so on. Therefore, the numerical effort is significantly increased for systems exhibiting non-trivial absorbing states and only small system sizes are available by simulations. But nevertheless convincing data-collapses, including the pair contact process data, are obtained and the corresponding universal scaling functions are shown in figure 7. The values of the exponents used are listed in table 1. In summary, activity spreading from a localized seed is characterized by the same universal scaling functions \tilde{P}_{pbc} and \tilde{N}_{pbc} for all considered models. Thus the CP, sDP, and especially the PCP display the same dynamical scaling behavior at criticality.

5 Conclusions

Similar to equilibrium critical phenomena, the great variety of non-equilibrium phase transitions can be grouped into different universality classes. Each non-equilibrium universality class is characterized by a certain symmetry which is often masked within the Langevin equation approach, but it is expressed clearly within the corresponding path integral formulation (see e.g. [2,15] and references therein). For example, non-equilibrium critical systems belong to the directed percolation universality class if the associated absorbing phase transition is described by a single component order parameter and if the corresponding coarse grained system obeys the rapidity reversal symmetry (at

least asymptotically). This is clearly demonstrated in figure 2 where the data of five different models is shown. Although the models exhibit different interaction details their rescaled data collapse onto a unique universal scaling curve. This scaling plot is an impressive manifestation of the robustness of the DP universality class. On the other hand, it allows the identification of the irrelevant parameters, i.e., those parameters which do not affect the universality class. As expected, the used update scheme, the lattice structure and the different implementation schemes of the conjugated field do not affect the scaling behavior. But it is worth mentioning that the structure of the absorbing phase was considered so far as a relevant parameter. For example, it was expected that models with infinitely many absorbing states belong to a different universality class than DP. The observed (steady state and dynamical) DP-scaling behavior of the pair contact process at criticality reveals that the number of absorbing states does not contribute to the asymptotic scaling behavior at criticality. For the sake of completeness, we mention that different universality classes than DP occur if the rapidity reversal is broken, e.g. by quenched disorder [1,76–81], or additional symmetries [3,4] such as particle-hole symmetry (compact directed percolation [30,82]), or particle conservation (Manna universality class [83,84,57]) or parity conservation (for example branching annihilating random walks with an even number of offsprings [85,86]).

We would like to thank P. Grassberger for communicating his results prior to publication. Furthermore, we thank H.-K. Janssen for instructive discussions and useful comments on the manuscript.

References

- [1] H. Hinrichsen, *Adv. Phys.* **49**, 815 (2000).
- [2] G. Ódor, *Rev. Mod. Phys.* **76**, 663 (2004).
- [3] H. K. Janssen, *Z. Phys. B* **42**, 151 (1981).
- [4] P. Grassberger, *Z. Phys. B* **47**, 365 (1982).
- [5] T. Ohtsuki and T. Keyes, *Phys. Rev. A* **35**, 2697 (1987).
- [6] T. Ohtsuki and T. Keyes, *Phys. Rev. A* **36**, 4434 (1987).
- [7] H. Mori and K. J. Mc Neil, *Prog. Theor. Phys.* **57**, 770 (1977).
- [8] H. K. Janssen and U. C. Täuber, *Ann. Phys.* **315**, 147 (2005).
- [9] U. C. Täuber, M. Howard, and B. P. Vollmayr-Lee, *J. Phys. A* **38**, R79 (2005).
- [10] H. K. Janssen, *J. Stat. Phys.* **103**, 801 (2001).
- [11] C. J. De Dominicis, *J. Phys. C (France)* **37**, 247 (1976).

- [12] H. K. Janssen, Z. Phys. B **23**, 377 (1976).
- [13] P. C. Martin, E. D. Siggia, and H. A. Rose, Phys. Rev. A **8**, 423 (1973).
- [14] H. D. I. Abarbanel, J. B. Bronzan, R. L. Sugar, and A. R. White, Phys. Rep. **21**, 119 (1975).
- [15] H. K. Janssen, cond-mat/0304631 (2004).
- [16] S. Lübeck, Int. J. Mod. Phys. B **18**, 3977 (2004).
- [17] H. K. Janssen, Ü. Kutbay, and K. Oerding, J. Phys. A **32**, 1809 (1999).
- [18] H. K. Janssen and O. Stenull, Phys. Rev. E **69**, 016125 (2004).
- [19] S. Lübeck and R. D. Willmann, J. Stat. Phys. **115**, 1231 (2004).
- [20] H. K. Janssen, B. Schaub, and B. Schmittmann, Z. Phys. B **71**, 377 (1988).
- [21] S. Lübeck and H. K. Janssen, Phys. Rev. E , (2005).
- [22] P. Grassberger, private communication , (2004).
- [23] J. F. Nicoll and P. C. Albright, Phys. Rev. B **31**, 4576 (1985).
- [24] E. Barouch, B. M. McCoy, and T. T. Wu, Phys. Rev. Lett. **31**, 1409 (1973).
- [25] G. Delfino, Phys. Lett. B **419**, 291 (1998).
- [26] S. Lübeck and R. D. Willmann, J. Phys. A **35**, 10205 (2002).
- [27] An instructive example is known from equilibrium. Whereas the critical exponents of the three-dimensional Ising, XY, and Heisenberg universality class differ slightly certain amplitude combinations differ by a factor 1.5 or even by more than a factor 2 (see [28] for an overview). Note that amplitude combinations are just particular values of corresponding scaling functions.
- [28] V. Privman, P. C. Hohenberg, and A. Aharony, in *Universal critical-point amplitude relations in Phase Transitions and Critical Phenomena, Vol. 14*, edited by C. Domb and J. L. Lebowitz (Academic Press, London, 1991).
- [29] T. M. Liggett, *Interacting particle systems* (Springer, New York, 1985).
- [30] E. Domany and W. Kinzel, Phys. Rev. Lett. **53**, 311 (1984).
- [31] I. Jensen, Phys. Rev. Lett. **70**, 1465 (1993).
- [32] J. F. F. Mendes, R. Dickman, M. Henkel, and M. C. Marques, J. Phys. A **27**, 3019 (1994).
- [33] R. M. Ziff, E. Gularí, and Y. Barshad, Phys. Rev. Lett. **56**, 2553 (1986).
- [34] J. Marro and R. Dickman, *Nonequilibrium phase transitions in lattice models* (Cambridge University Press, Cambridge, 1999).
- [35] S. Lübeck and P. C. Heger, Phys. Rev. E **68**, 056102 (2003).

- [36] P. Grassberger, *J. Phys. A* **22**, 3673 (1989).
- [37] P. Grassberger and Y.-C. Zhang, *Physica A* **224**, 169 (1996).
- [38] E. Carlon, M. Henkel, and U. Schollwöck, *Phys. Rev. E* **63**, 036101 (2001).
- [39] I. Jensen, *J. Phys. A* **29**, 7013 (1996).
- [40] I. Jensen and R. Dickman, *Phys. Rev. E* **48**, 1710 (1993).
- [41] R. Dickman, [cond-mat/9909347](http://arxiv.org/abs/cond-mat/9909347) (1999).
- [42] R. Dickman and J. Kamphorst Leal da Silva, *Phys. Rev. E* **58**, 4266 (1998).
- [43] R. Dickman, W. Rabelo, and G. Ódor, *Phys. Rev. E* **65**, 016118 (2001).
- [44] M. A. Muñoz, G. Grinstein, R. Dickman, and R. Livi, *Phys. Rev. Lett.* **76**, 451 (1996).
- [45] F. van Wijland, *Phys. Rev. Lett.* **89**, 190602 (2002).
- [46] F. van Wijland, *Braz. J. Phys.* **33**, 551 (2003).
- [47] P. Grassberger, *Math. Biosci.* **63**, 157 (1983).
- [48] J. L. Cardy and P. Grassberger, *J. Phys. A* **18**, L267 (1985).
- [49] H. K. Janssen, *Z. Phys. B* **58**, 311 (1985).
- [50] G. Ódor, J. M. Mendes, M. A. Santos, and M. C. Marques, *Phys. Rev. E* **58**, 7020 (1998).
- [51] J. Kamphorst Leal da Silva and R. Dickman, *Phys. Rev. E* **60**, 5126 (1999).
- [52] I. Jensen, H. C. Fogedby, and R. Dickman, *Phys. Rev. A* **41**, 3411 (1990).
- [53] G. Grinstein, Z. W. Lai, and R. J. Browne, *Phys. Rev. A* **40**, 4820 (1989).
- [54] C. A. Voigt and R. M. Ziff, *Phys. Rev. E* **56**, R6241 (1997).
- [55] D.-J. Liu, N. Pavlenko, and J. W. Evans, *J. Stat. Phys.* **114**, 101 (2004).
- [56] V. Privman and M. E. Fisher, *Phys. Rev. B* **30**, 322 (1984).
- [57] S. Lübeck and P. C. Heger, *Phys. Rev. Lett.* **90**, 230601 (2003).
- [58] W. Kinzel, *Z. Phys. B* **58**, 229 (1985).
- [59] T. Tomé, *Physica A* **212**, 99 (1994).
- [60] H. Rieger, A. Schadschneider, and M. Schreckenberg, *J. Phys. A* **27**, L423 (1994).
- [61] A. P. F. Atman, R. Dickman, and J. G. Moreira, *Phys. Rev. E* **67**, 016107 (2003).
- [62] S. P. Obukhov, *Physica A* **101**, 145 (1980).
- [63] J. L. Cardy and R. L. Sugar, *J. Phys. A* **13**, L423 (1980).

- [64] N. Aktekin, *J. Stat. Phys.* **104**, 1397 (2001).
- [65] D. Grüneberg and A. Hucht, *Phys. Rev. E* **69**, 036104 (2004).
- [66] P. Grassberger, (2004).
- [67] P. Grassberger and A. de la Torre, *Ann. Phys. (N.Y.)* **122**, 373 (1979).
- [68] H. K. Janssen, B. Schaub, and B. Schmittmann, *Z. Phys. B* **73**, 539 (1988).
- [69] C.-K. Hu, C.-Y. Lin, and J.-A. Chen, *Phys. Rev. Lett.* **75**, 193 (1995).
- [70] K. Kaneda, Y. Okabe, and M. Kikuchi, *J. Phys. A* **32**, 7263 (1999).
- [71] K. Kaneda and Y. Okabe, *Phys. Rev. Lett.* **86**, 2134 (2001).
- [72] A. Hucht, *J. Phys. A* **35**, L481 (2002).
- [73] T. Antal, M. Droz, and Z. Rácz, *J. Phys. A* **37**, 1465 (2004).
- [74] I. Jensen, *J. Phys. A* **32**, 5233 (1999).
- [75] I. Jensen, *Phys. Rev. A* **45**, R563 (1992).
- [76] H. K. Janssen, *Phys. Rev. E* **55**, 6253 (1997).
- [77] I. Jensen, *Phys. Rev. Lett.* **77**, 4988 (1996).
- [78] A. G. Moreira, *Phys. Rev. E* **54**, 3090 (1996).
- [79] R. Cafiero, A. Gabrielli, and M. A. Muñoz, *Phys. Rev. E* **57**, 5060 (1998).
- [80] J. Hooyberghs, F. Iglói, and C. Vanderzande, *Phys. Rev. E* **69**, 066140 (2004).
- [81] T. Vojta, *Phys. Rev. E* **70**, 026108 (2004).
- [82] J. W. Essam, *J. Phys. A* **22**, 4927 (1989).
- [83] S. S. Manna, *J. Phys. A* **24**, L363 (1991).
- [84] M. Rossi, R. Pastor-Satorras, and A. Vespignani, *Phys. Rev. Lett.* **85**, 1803 (2000).
- [85] D. Zhong and D. ben Avraham, *Phys. Lett. A* **209**, 333 (1995).
- [86] J. L. Cardy and U. C. Täuber, *Phys. Rev. Lett.* **13**, 4780 (1996).